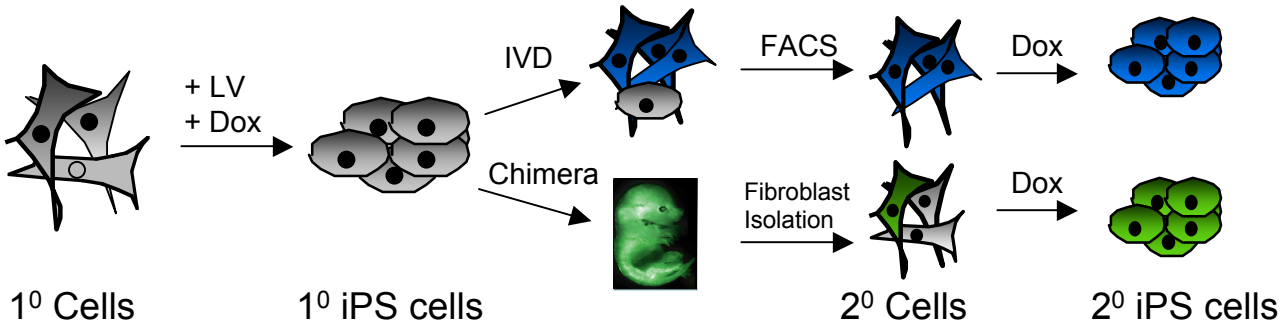

Supplementary Figure 1

a

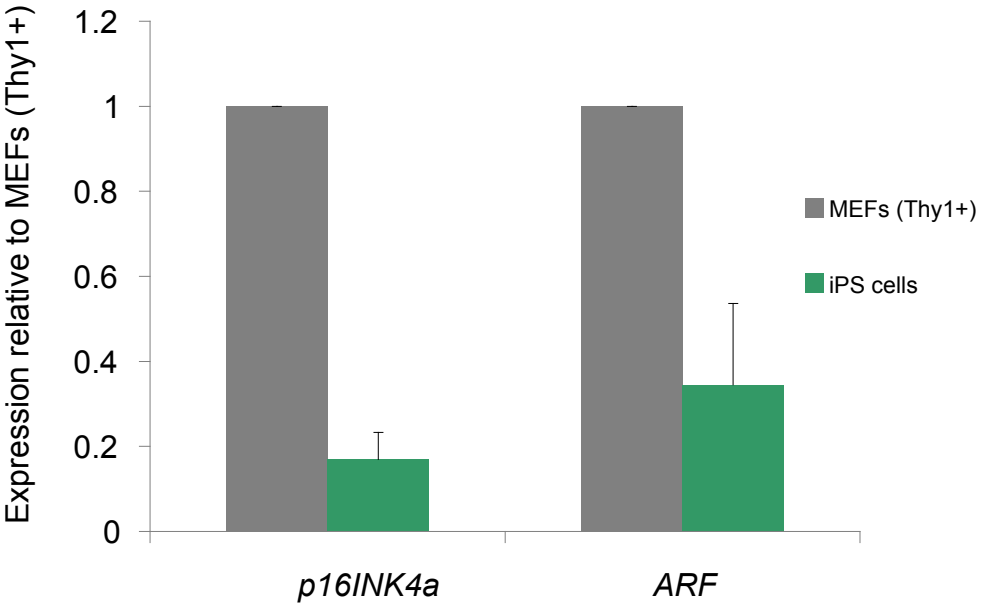

b

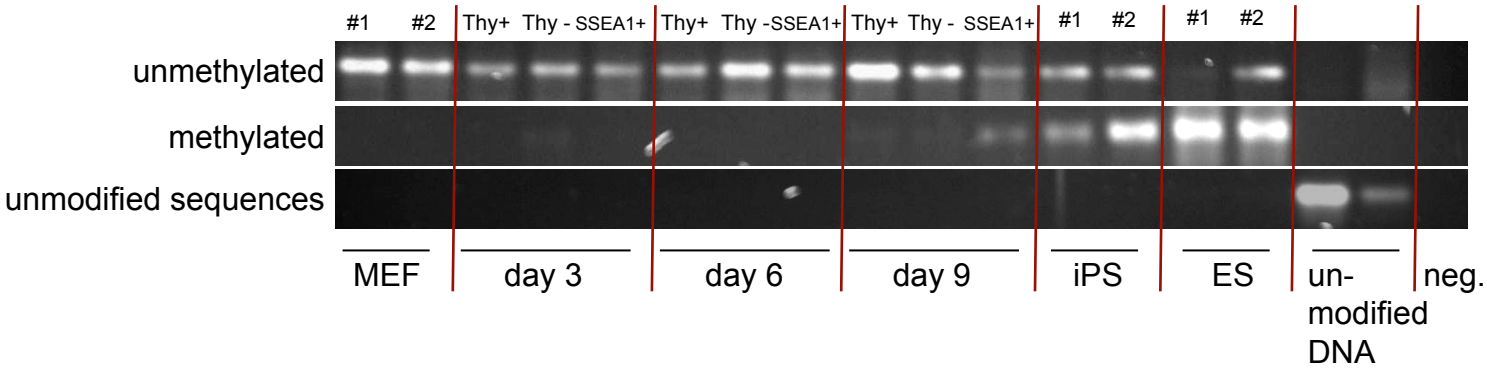

Supplementary Figure 2

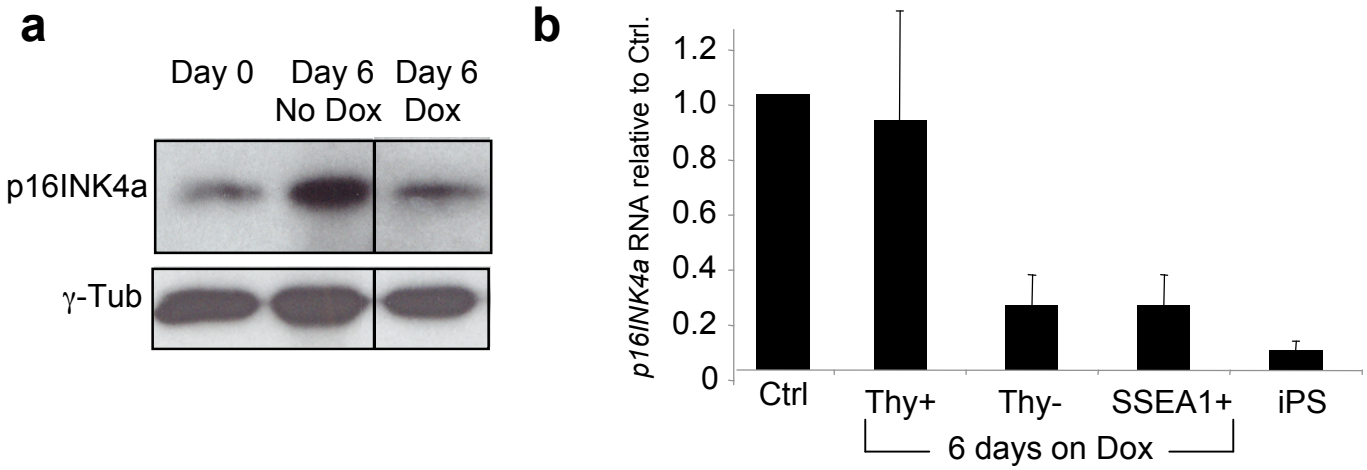

Supplementary Figure 3

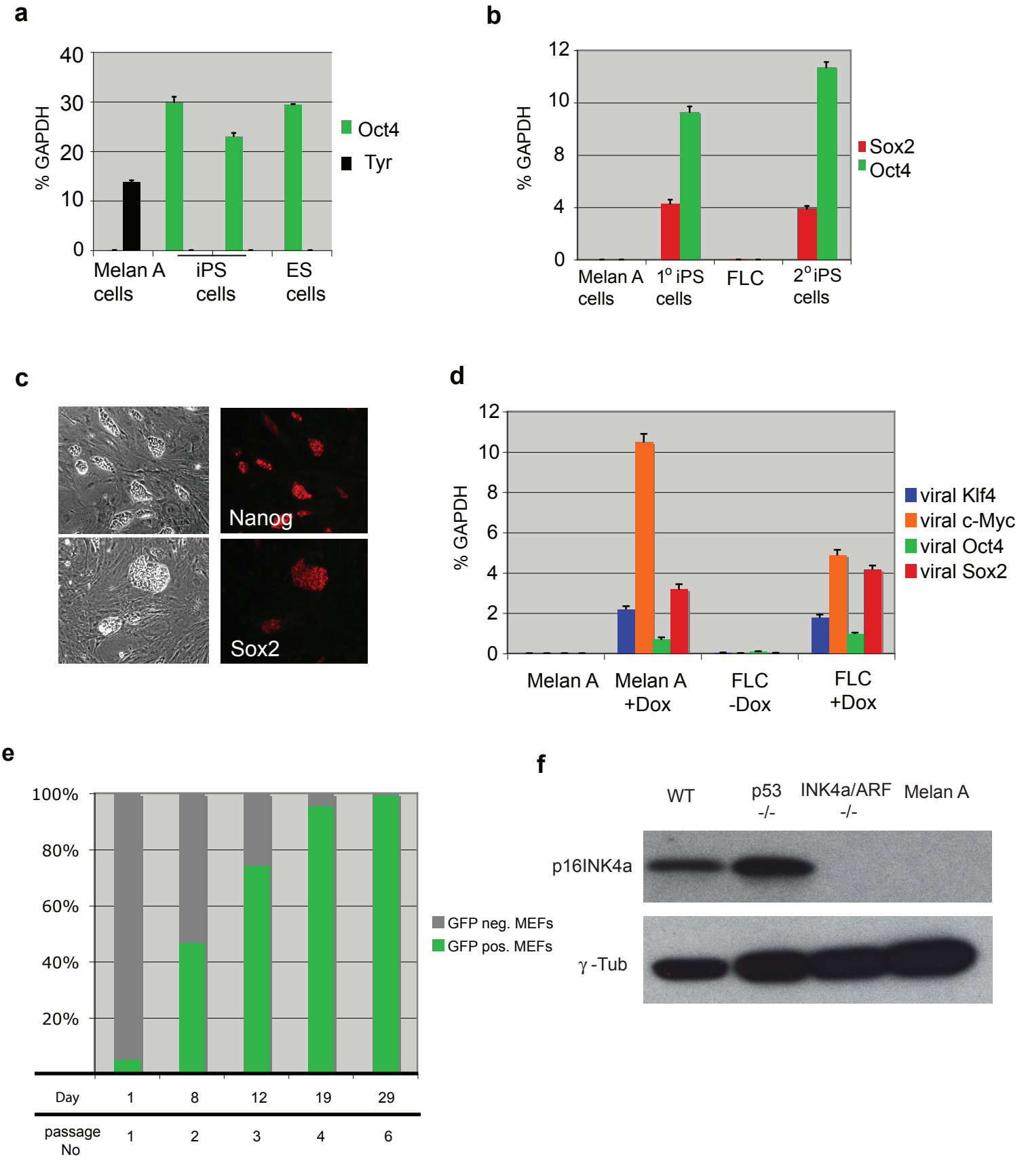

Supplementary Figure 4

a

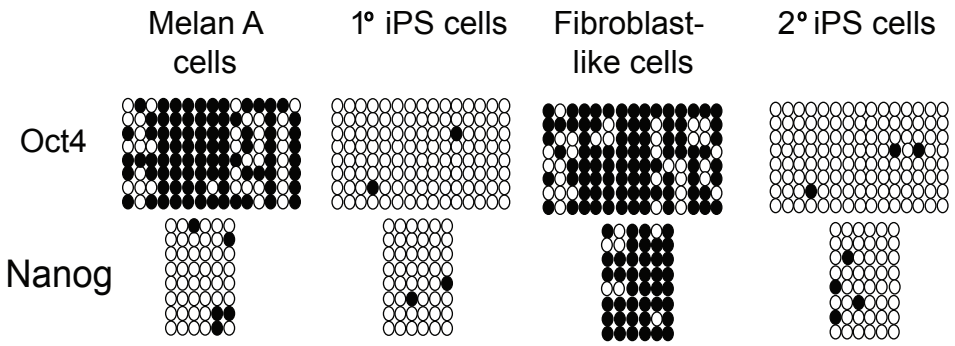

b

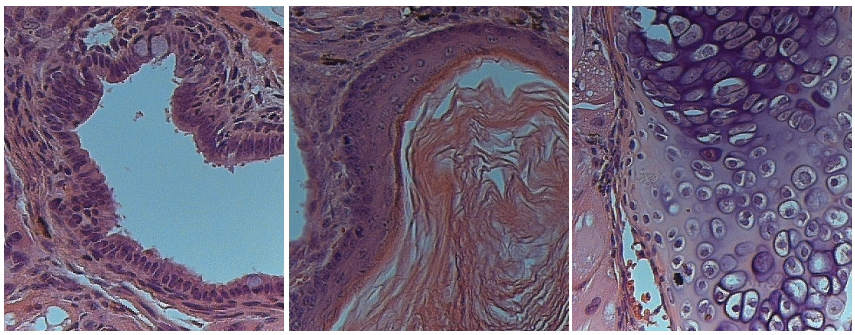

Endoderm Ectoderm Mesoderm

Supplementary Figure 5

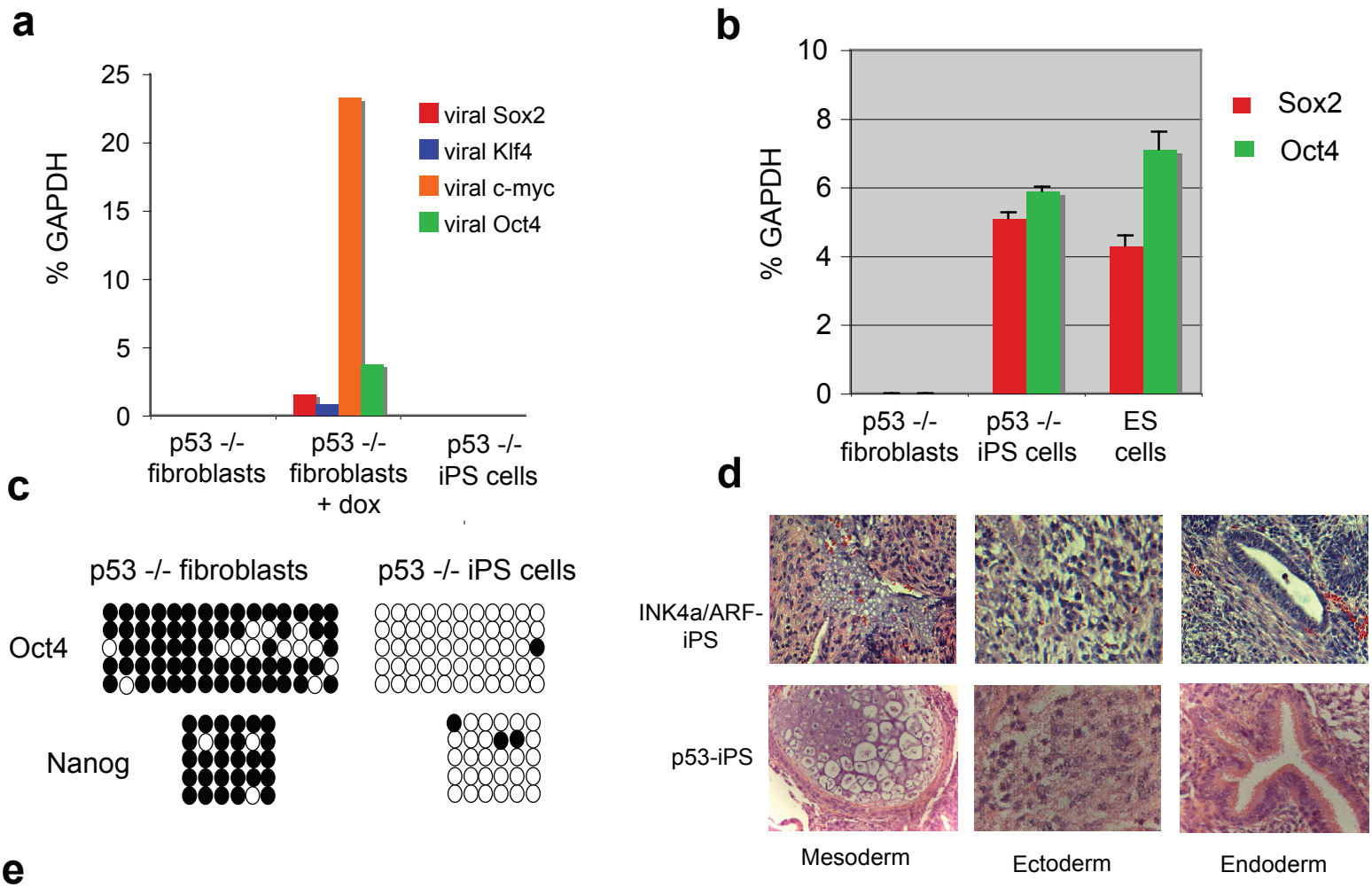

Supplementary Figure 6

a

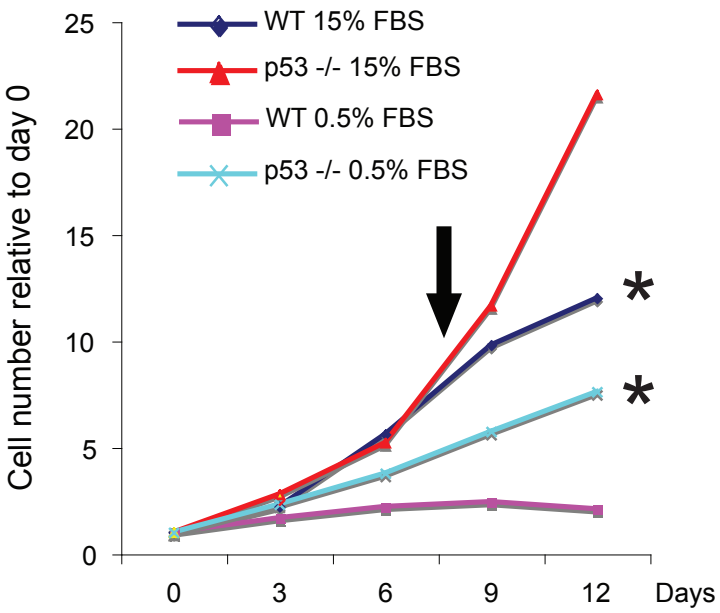

b

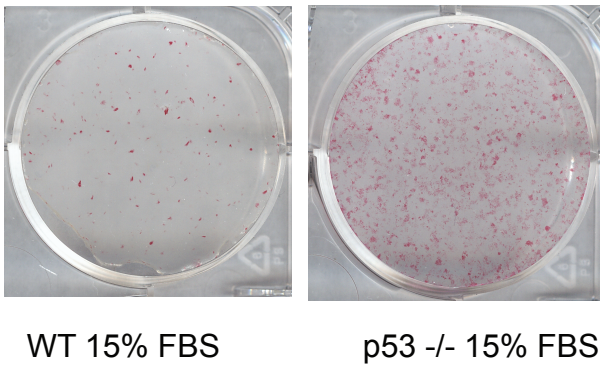

c

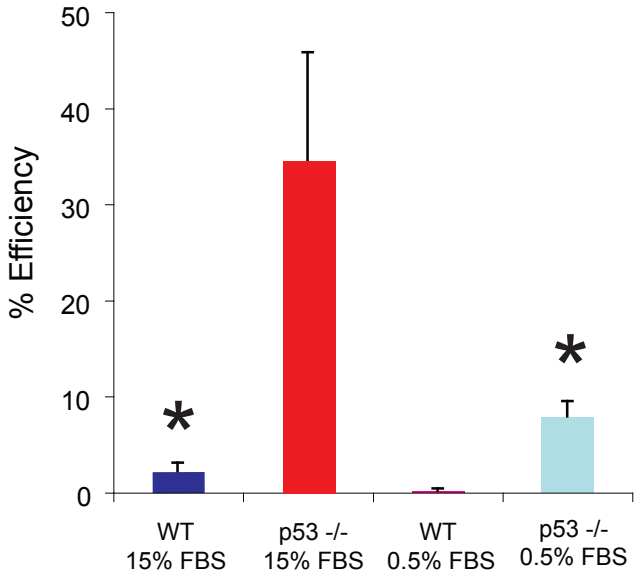

Supplementary Figure 7

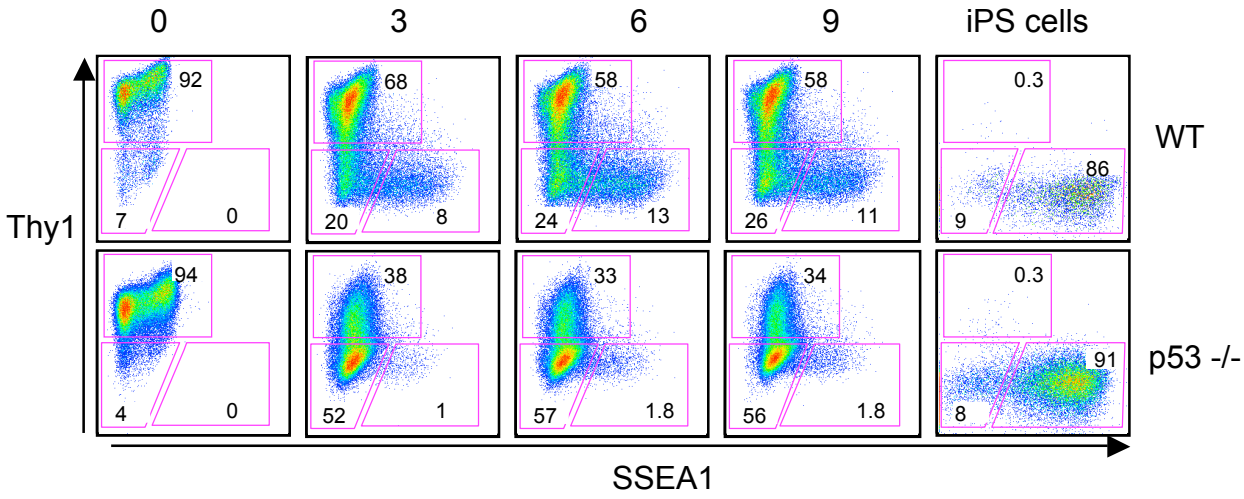

Supplementary Figure 8

a

β-gal Staining

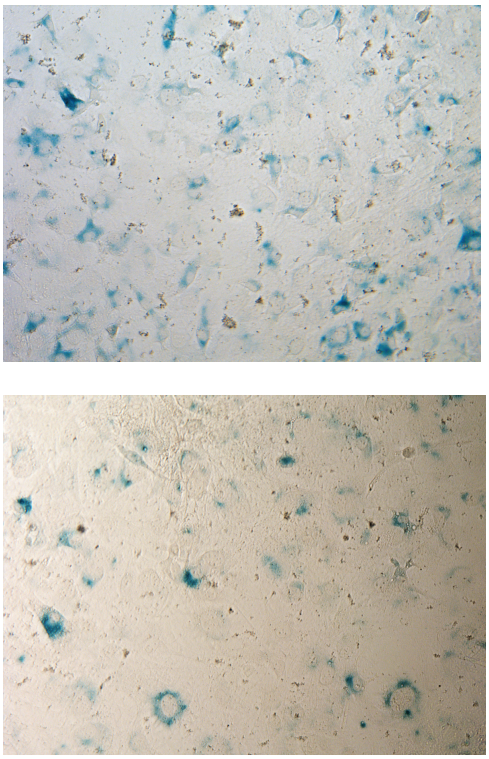

MEFs (p5)

MEFs (p5)
+ shp53

b

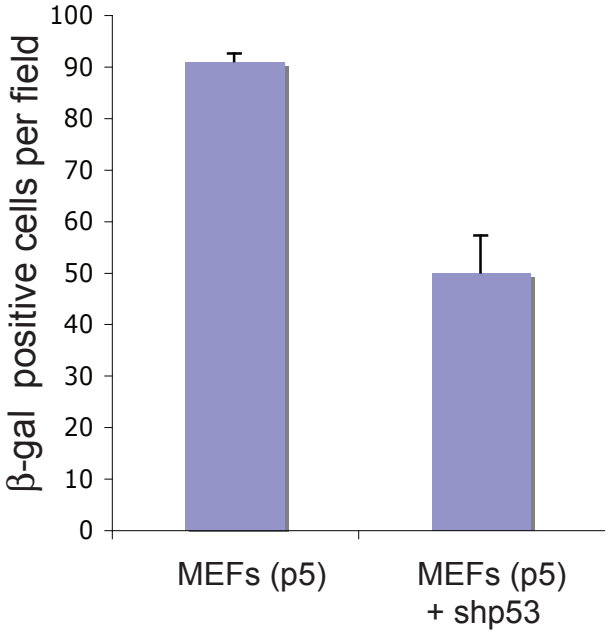

c

AP Staining

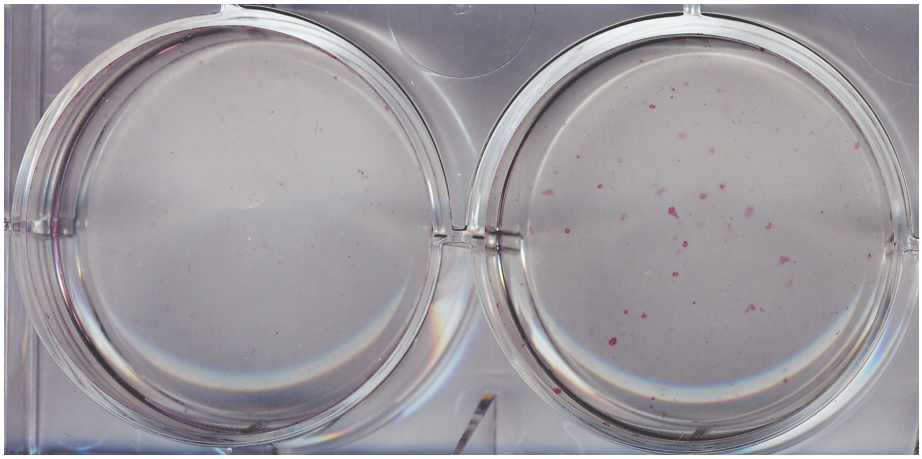

MEFs (p5)

MEFs (p5) + shp53

Supplementary Figure 9

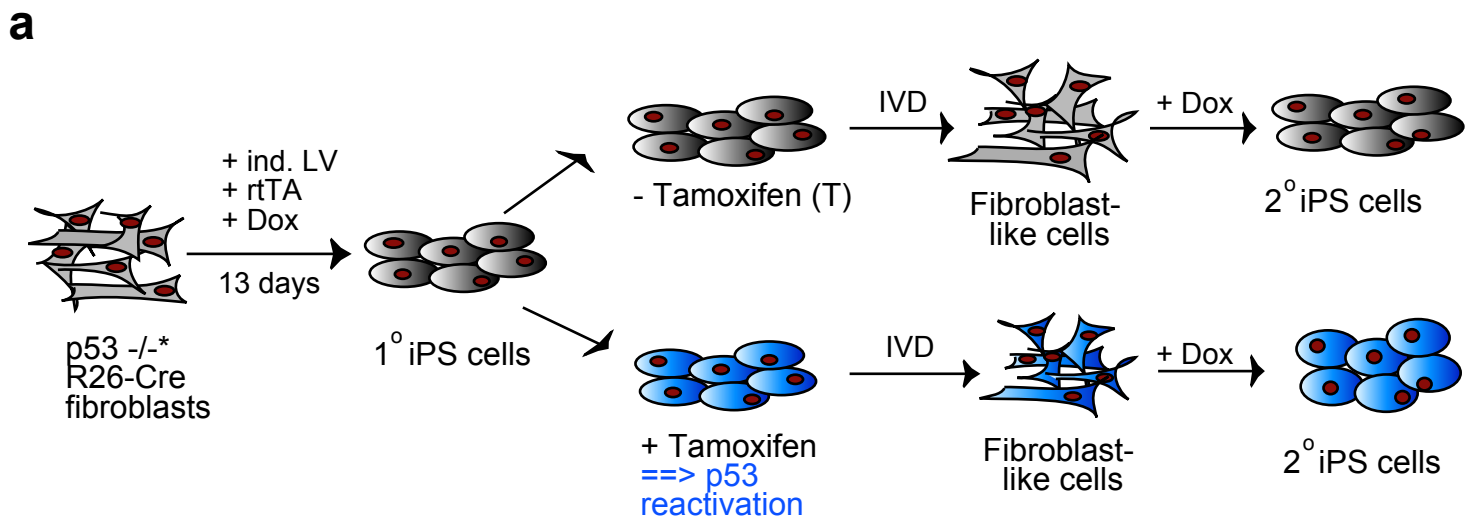

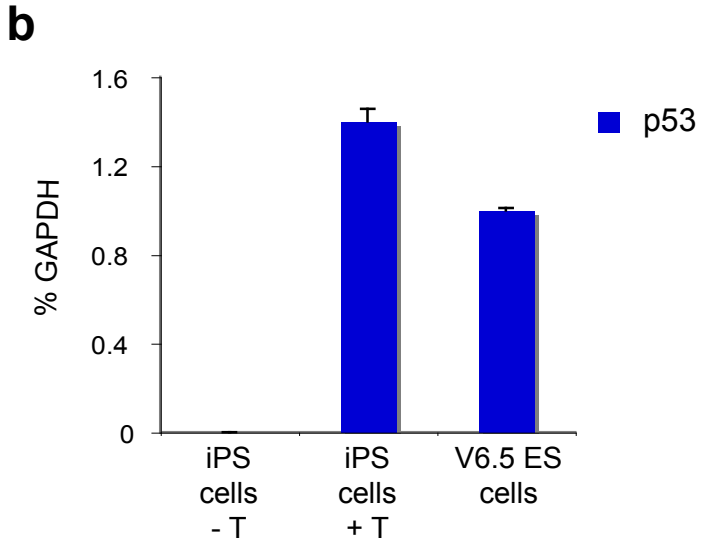

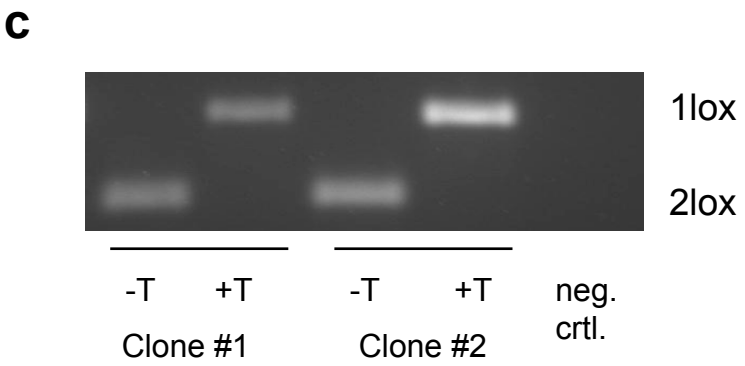

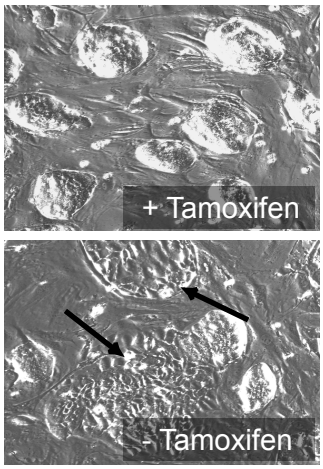

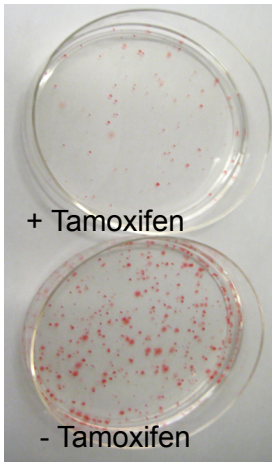

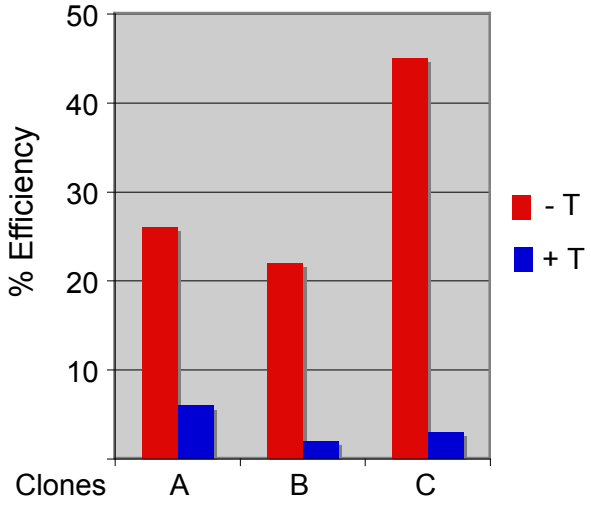

Supplementary Figure 10

a

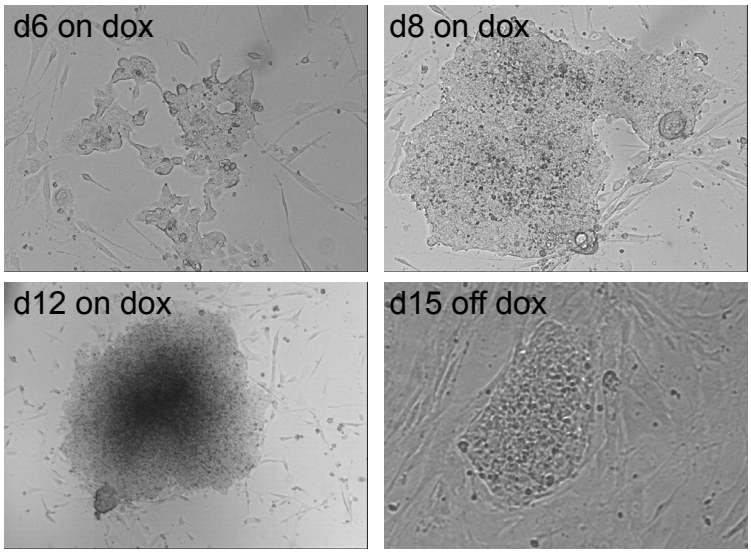

b

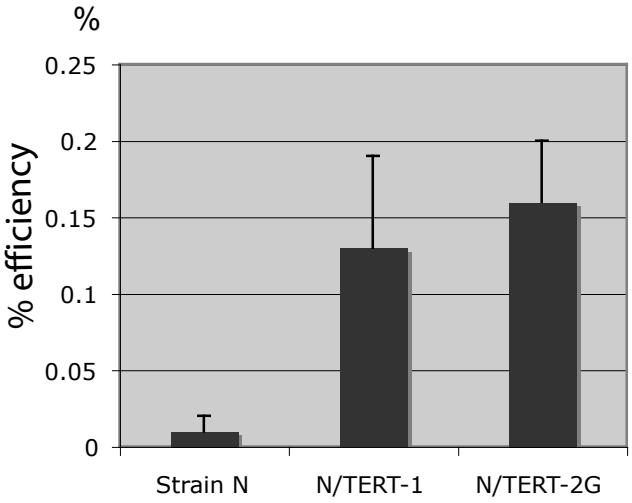

c

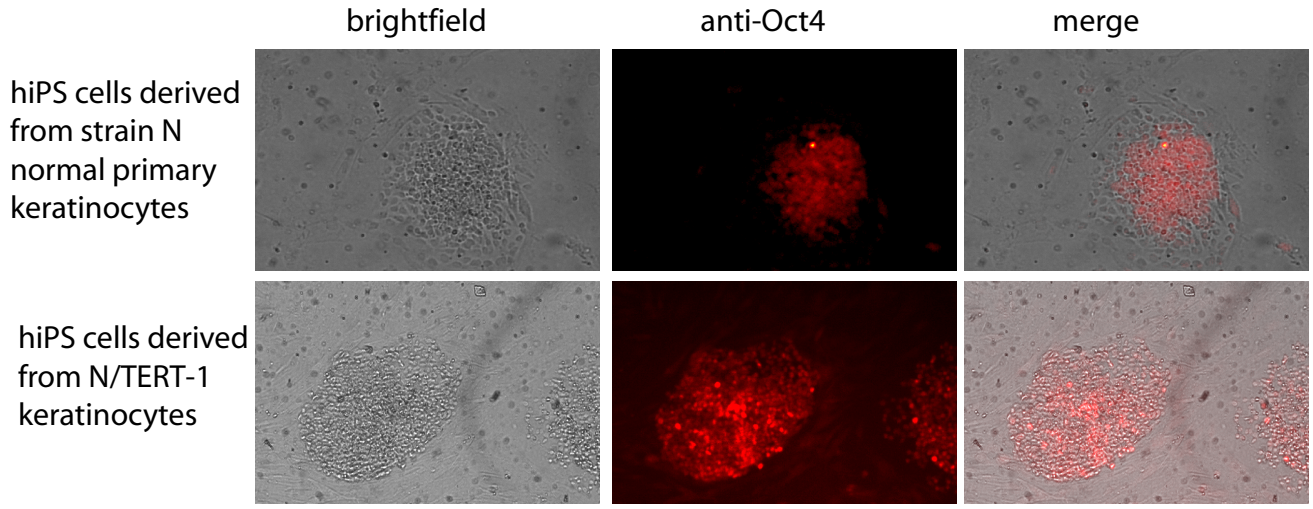

Supplementary Figure 11

Supplementary Table 1: Karyotypes of varius iPS cell lines.

Nomenclature	Cells	Results
11p5subclone	Melan A cells	Trisomy 6 plus randon chromosome gain and loss.
9p3	Melan A iPS 57	Very heterogenous and unstable with various abnormalities.
10p3	Melan A iPS 59	Half hyperdiploid, half hypertetraploid (near octoploid). Trisomy 6 and 8.
12p10	p53 -/-	All cells polyploid with ~80% tetraploid. Loss of 1 plus other abnormalities.
1p4	p53 -/- iPS #1	Hypotetraploid (66-73). Balanced 4/Y translocation
3p4	p53 -/- iPS #2	Tetraploid (72-80 chrom.). Same 4/Y translocation as 1p4.
5p4	p53 -/- iPS #3	Diploid (40-42). Unstable. Same 4/Y translocation as 1p4.
2p4	p53 -/- iPS #1+ Tamoxifen	36% with unstabled hypertetraploid karyotype. Same 4/Y translocation as 1p4.
4p4	p53 -/- iPS #2+ Tamoxifen	Hypotetraploid (68-75)). Balanced 4/Y translocation. Very similar to 1p4
6p4	p53 -/- iPS #3+ Tamoxifen	Tetraploid (70-75 chrom.). Same 4/Y translocation as 1p4, plus others.
13p10	INK4A/ARF MEF	>90% polyploid plus other abnormalities. Both male and female clone present.
7p3	INK4A/ARF iPS #1	2 clones. Fewer abnormalities than 1-6. X loss, extra material in C3, deletion in X.
8p3	INK4A/ARF iPS #2	3 clones, all with distinct abnormalities (loss of X, gain of 8). Similar to 7p3.

Supplementary Table 2: primer sequences used for PCR analysis

Gene	**Forward primer** (5' to 3')	**Reverse primer** (5' to 3')
GAPDH	AGGTCGGTGTGAACGGATTTG	TGTAGACCATGTAGTTGAGGTCA
Dopachrome Tautomerase	CTAACCGCAGAGCAACTTGG	CAAGAGCAAGACGAAAGCTCC
Nanog	TTGCTTACAAGGGTCTGCTACT	ACTGGTAGAAGAATCAGGGCT
Tyrosinase	AGTTTACCCAGAAGCCAATGC	CGACTGGCCTTGTTCCAAGT
Klf4 (endogenous)	AACATGCCCGGACTTACAAA	TTCAAGGGAATCCTGGTCTTC
c-Myc (endogenous)	TAACTCGAGGAGGAGCTGGA	GCCAAGGTTGTGAGGTTAGG
Oct4 (endogenous)	TAGGTGAGCCGTCTTTCCAC	GCTTAGCCAGGTTCGAGGAT
Sox2 (endogenous)	TTAACGCAAAAACCGTGATG	GAAGCGCCTAACGTACCACT
c-Myc (lentiviral)	AAGAGGACTTGTTGCGGAAA	TTGTAATCCAGAGGTTGATTATCG
Klf4 (lentiviral)	ATGGTCAAGTTCCCAGCAAG	TGATATCGAATTCCGTTTGTTT
Oct4 (lentiviral)	GCTCGTTTAGTGAACCGTCAG	CGAAGTCTGAAGCCAGGTGT
Sox2 (lentiviral)	GGCCATTAACGGCACACT	AAGCAGCGTATCCACATAGC
p21	TTGCACTCTGGTGTCTGAGC	TGCGCTTGGAGTGATAGAAA
p16INK4A	GTGTGCATGACGTGCGGG	GCAGTTCGAATCTGCACCGTAG
p19Arf	GCTCTGGCTTTCGTGAACATG	TCGAATCTGCACCGTAGTTGAG

Supplementary Table 2

Supplementary Figure 1. Scheme of secondary (2^o) cell generation from iPS cells. Primary (1^o) cells were infected with polycistronic lentivirus (LV) in the presence of doxycycline (Dox) to produce 1^o iPS cells, which were either in vitro differentiated (IVD) into $Thy1^+$, $Flk1^+$, $SSEA1^-$ fibroblast-like 2^o cells, or labeled with lentivirus constitutively expressing GFP and injected into blastocysts to recover 2^o murine embryonic fibroblasts (MEFs) at E14.5.

Supplementary Figure 2. Silencing of the *INK4a/ARF* locus in iPS cells.
(a) RT-qPCR for *p16INK4a* and *ARF* in MEF and derivative iPS cells. Note the low expression levels of of both genes in iPS cells when compared to MEFs. **(b)** Methylation specific PCR of the INK4a/ARF locus in MEFs, intermediate cell populations, iPS cells and ES cells. Note that methylation of the locus occurs only in the $SSEA1^+$ intermediates isolated at day 9 and remains methylated in iPS cells. Control ES cells also show strong methylation of the locus.

Supplementary Figure 3. Downregulation of p16INK4a during reprogramming.
(a) Downregulation of p16INK4a in bulk population of secondary MEFs exposed to doxycycline for 6 days, as determined by Western blot analysis. **(b)** Downregulation of *p16INK4a* transcript in $Thy1^-$ and $SSEA1^+$ subpopulations after 6 days of transgene expression

Supplementary Figure 4. Molecular and functional characterization of Melan A-derived secondary cells.
(a) qPCR for the melanocyte marker tyrosinase (Tyr) and the pluripotency marker Oct4 in Melan A cells, two independently derived iPS clones and control ES cells. ND = not detected. **(b)** qPCR for Oct4 and Sox2 in Melan A cells, primary iPS cells, fibroblast-like secondary cells (FLC) and resultant secondary iPS cells. Note the absence of pluripotency markers in somatic cells and their activation upon conversion into iPS cells. **(c)** Immunofluorescence images for Nanog and Oct4 of iPS colonies derived from Melan A cells. **(d)** qPCR for viral transgene expression in Melan A cells and secondary FLC in the presence of doxycycline. Note the absence of transgene expression in the absence of

doxycycline induction. **(e)** Growth behavior of GFP^+ (iPS cell-derived) and GFP^- (host blastocyst-derived) MEFs was determined by flow cytometry at different passages until day 29. Note the selective growth advantage of GFP^+ over GFP^- MEFs over time. **(f)** Western blot analysis for p16INK4a in wild type (WT) fibroblasts, *p53*-/- fibroblasts, *INK4a/ARF*-/- fibroblasts and Melan A cells (γ-tubulin was used as loading control).

Supplementary Figure 5. Promoter methylation and developmental potential in Melan A-derived cells.

(a) Methylation status of the Oct4 and Nanog promoters in the indicated cell populations as assessed by bisulfite sequencing. Black circles represent methylated cytosines while open circles represent unmethylated cytosines. **(b)** Hematoxylin and Eosin stained teratoma section produced from secondary Melan A- derived iPS cell clone. Note differentiation into structures indicative of ectodermal (keratinized epithelium), endodermal (glandular structures) and mesodermal (cartilage) tissues.

Supplementary Figure 6. Molecular and functional characterization of *p53* and *INK4a/ARF*-deficient fibroblasts.

(a) qPCR for viral transgene expression in untreated *p53*-/- fibroblasts, virally infected fibroblasts in the presence of doxycycline and derivative stable iPS cells upon discontinuation of doxycycline. **(b)** qPCR for endogenous Oct4 and Sox2 indicates expression of these markers in *p53*-/- iPS cells at levels comparable to WT ES cells. **(c)** Bisulfite methylation analysis of Oct4 and Nanog promoters in p53-/- fibroblasts and derivative iPS cells. Note promoter demethylation in iPS cells. **(d)** Differentiation potential of *p53*- and *INK4a/ARF*-deficient iPS cells as assessed by teratoma formation. Shown are typical endodermal, mesodermal and ectodermal structures. **(e)** Immunofluorescence for tdTomato of a newborn pup produced with *p53*-/- iPS cells that have been labeled with a lentivirus constitutively expressing tdTomato. Note contribution of iPS cells to different tissues (brain, lung, tongue). **(f)** $tdTomato^+$ MEFs isolated from *p53*-/- iPS cell-derived E13.5 chimera. **(g)** $tdTomato^+$ MEFs isolated from *INK4a/ARF*-/- iPS cell-derived E13.5 chimera. **(h)** Chimeric pup produced from *p53*-/- iPS cells and non-chimeric control pup. Black arrow denotes exencephaly.

Supplementary Figure 7. Enhanced reprogramming potential of immortal cells depends on long-term growth potential, not actual growth rate.

(a) Growth curves of WT and p53-/- MEFs cultured in either low (0.5%) or high (15%) serum. **(b)** AP staining of iPS cell colonies derived from 4-factor-infected WT and p53-/- MEFs induced with doxycyline for 8 days, when growth rates are still comparable (black arrow in (a)); colonies were scored on day 13. Note that WT and p53-/- MEFs show different reprogramming potentials despite similar growth rates. **(c)** Reprogramming efficiencies of p53-/- and WT MEFs cultured in low and high serum. Note increased reprogramming potential of p53-/- MEFs grown at 0.5% serum over WT cells grown at 15% (relevant bars marked by asterisks) despite higher growth rate of WT cells over p53-/- cells (see curves in (a), marked by asterisks).

Supplementary Figure 8. Reprogramming kinetics in WT and p53-/- cells.

FACS analysis for $Thy1^+$ and $SSEA1^+$ subpopulations appearing in WT and p53-/- MEFS at days 0, 3, 6 and 9 after transgene expression.

Supplementary Figure 9. Acute inactivation of p53 endows senescent cultures with reprogramming potential.

(a) Shown are secondary MEFs at passage 5 stained for senescence-associated β-galactosidase in the presence of shp53 or a control vector. **(b)** Quantification of β-galactosidase positive cells. **(c)** AP staining of iPS cell-like colonies emerging from control vector or shp53-infected secondary cells. Note that senescent cultures treated with shp53 can overcome the reprogramming block to generate iPS cell colonies. AP staining was performed 5 days after withdrawal of doxycycline from cultures to ensure transgene-independent self-renewal.

Supplementary Figure 10. Continuous p53 deficiency is required for enhanced reprogramming efficiency.

(a) Schematic representation of p53 reactivation experiment. Tail-tip fibroblasts from a mouse carrying a conditionally reactivatable p53 allele (designated "-*" allele) and a

constitutive null allele (designated "-" allele) as well as a ROSA26 promoter driven tamoxifen-inducible CreER allele were infected with the four doxycycline-inducible lentiviruses to produce primary iPS cells. Treatment of iPS cell clones with tamoxifen resulted in the reactivation of one p53 allele (designated "+" allele). Subsequent in vitro differentiation (IVD) yielded secondary cells, which converted into secondary iPS cells upon treatment with doxycycline. **(b)** qPCR for p53 transcript in untreated (-T) iPS cells and iPS cells treated with tamoxifen (+T) in comparison with V6.5 control ES cells. **(c)** PCR to detect reactivation of conditional p53 allele in iPS cells obtained from p53-/-*, ROSA26-CreER tail fibroblasts. Shown are two independently derived iPS cell clones in the presence or absence of tamoxifen. 1lox denotes successfully excised STOP cassette, which indicates reactivation of the wild type p53 allele while 2lox denotes non-excised non-functional allele. **(d)** Representative colonies of p53-/-* iPS cell colonies before and after tamoxifen treatment. Note the disappearance of differentiated colonies upon reactivation of p53. This is likely due to the loss of iPS cell-derived differentiated cells that had a growth advanatge in the absence of p53. **(e)** AP staining of plates seeded with secondary cells from tamoxifen-treated (p53+/-) or untreated (p53-/-) iPS cells. **(f)** Reprogramming efficiencies of secondary cells derived from tamoxifen-treated (p53+/-) or untreated (p53-/-) iPS cells.

Supplementary Figure 11. hTERT-immortalized human keratinocytes yield more iPS-like colonies than primary keratinocytes.

(a) N/TERT immortalized keratinocytes cell line (N/TERT-1) was co-infected with a polysistronic doxycycline-inducible lentivirus and a lentivirus constitutively expressing rtTA and the appearance of colonies was followed over time. **(b)** Reprogramming efficiencies of two different N/TERT immortalized keratinocyte cell lines (N/TERT-1 and N/TERT2G) compared with strain N primary normal keratinocytes. **(c)** Immunofluorescence for Oct4 in iPS-like colonies derived from WT keratinocytes and N/TERT immortalized keratinocytes cell line (N/TERT-1).